Anal. Bioanal. Electrochem., Vol. 12, No. 3, 2020, 402-414

Analytical &
Bioanalytical
Electrochemistry

2020 by CEE
www.abechem.com

Full Paper

Development of A New Electrochemical Sensor based on Zr-MOF/MIP for Sensitive Diclofenac Determination

Maryam Malekzadeh,[1] Alireza Mohadesi,[1,*] Mohammad Ali Karimi,[1] and Mehdi Ranjbar[2,*]

[1]*Department of Chemistry, Payame Noor University, P.O. Box 19395-4697 Tehran, Iran*
[2]*Pharmaceutics Research Center, Institute of Neuropharmacology, Kerman University of Medical Sciences, Kerman, Iran*

*Corresponding Author, Tel.: +983431325241; Fax: +983431325003
E-Mails: mehdi.Ranjbar@kmu.ac.ir; mohadesi@pnu.ac.ir

Received: 2 March 2020 / Accepted with minor revisions: 17 March 2020 /

Abstract- In this study, a new molecularly imprinted polymer with nanoporous material of zirconium metal-organic frameworks (Zr-MOF/MIP) for diclofenac (DFC) measurement is presented. The Zr-MOF/MIP was prepared by electropolymerization method, the Zr-MOFs were used to increase electrode surface and the DFC and para- aminobenzoic acid (pABA) were used as template and functional monomer, respectively. Zr--MOFs was characterized by using X-ray powder diffraction (XRD), scanning electron microscope (SEM) and Fourier transform infrared spectroscopy (FTIR). The electrochemical performance was investigated using cyclic voltammetry (CV) and differential pulse voltammetry (DPV). Sensor response was evaluated by comparing the electrochemical response of Zr-MOF/MIP, with that of non-Imprinted polymer (NIP), in a 2.0 mM potassium ferrocyanide solution containing 0.2 mM sodium sulfate as probe solution. Measurements were carried out in the potential range of -0.6 to +1.0 V with scan rate of 50 mV/s. The calibration curve of diclofenac was linear in the concentration range of 6.5 μM to $1.5\times10^{+3}$ μM. Detection limit was obtained 0.1 μM and relative standard deviation of several (n=7) replicate measurements for 1.0 mM DFC concentration has obtained 1.8%. Furthermore, favorable sensitivity, selectivity, good reproducibility and long-term stability, was obtained in the experiment and the proposed electrode was applied for the determination of DFC in pharmaceutical commercial sample with satisfactory results.

Keywords- Metal organic framework; Molecularly imprinted polymer; Electropolymerization; Diclofenac

1. INTRODUCTION

Non-steroidal anti-inflammatory drugs are one of the most widely used drugs in medical science. Diclofenac (DFC) as one of the anti-inflammatory drugs that prescribed for its effects such as pain relief, fever and treatment of diseases such as podagra, rheumatism, rheumatoid arthritis, osteoarthritis, pains of articulation and after operative pain. The unique properties of non-steroidal drugs are their non-opioid because they have anti-inflammatory properties, even at high doses. However, digestive problems such as diarrhea, peptic ulcer, nausea and allergic reactions such as dizziness, excretion of blood from the urine and headaches have been observed partly. Therefore, the identification and quantification of these drugs have been extensively studied in drug analytical laboratories [1,2]. Gas chromatography [3-6], spectrophotometry [7-10], mass spectrometry [11], liquid chromatography [12-16], high performance liquid chromatography [17,18], thin-layer chromatography [19-22], and flow injection spectrophotometry [23,24] have been reported for the determination of DFC in pharmaceutical formulations.

However, large instrument based approaches have some disadvantages such as: high associated costs, long working time and environmentally unfriendly. In the meantime, electrochemical methods have been validated due to their simplicity, low cost, short analysis time and high selectivity for the analysis of pharmaceutical formulations, and electrochemical sensors have been the focus of researchers due to their environmental compatibility [25-31].

Molecularly imprinted polymers (MIPs) serve as synthetic receptors for a wide variety of molecules and are synthesized using molecular imprinting techniques. MIPs have been used because of their specific properties in a variety of fields, including drug delivery [32], cell culture [33], catalyst [34,35] and biosensors [36-40].

In recent years, nanoporous materials of metal-organic frameworks (MOFs) consisting of inorganic metal clusters and organic molecules with coordination bonds have been used to develop the electrochemical sensors [41]. They have attracted much attention due to their structural properties, such as stable framework with high specific surface area, extremely high porosity, wide range of thermal, chemical stability, none-toxic nature, low density and pore volume.

In this paper, an electrochemical sensor was formed based on MIPs to determine the selectivity and based on MOFs to enhance the sensitivity for DFC measurement in real sample.

2. EXPERIMENTAL

2.1. Reagents and materials

The used chemicals such as para-amino benzoic acid (pABA), sodium sulfate, potassium ferrocyanide, sulfuric acid, ethanol, sodium hydroxide, zirconium sulfate, 2,6 pyridine dicarboxylic ammonium, cetyl trimethylammonium bromide (CTAB), DFC, sodium dehydrogenase phosphate and thiourea were purchased from Merck (Darmstadt, Germany). Alumina powder with dimension of 0.05 was purchased from Fluka (Buchs, Switzerland). Alfen X tablet is prepared from Alborz Co., Iran. Also all solutions were prepared with deionized water at room temperature. To remove dissolved oxygen, the cell solutions were purged with high-purity nitrogen.

2.2. Apparatus

All electrochemical experiments were performed using a polarograph that is connected to a PC via a USB port and NOVA 2.2 software (Metrohm, Model 797 VA computrance, Switzerland), using the three-electrode system: a GCE working electrode (d=2 mm, Azar Electrode Co.), a platinum auxiliary electrode, and an Ag/AgCl reference electrode. A pH meter (Metrohm, Model 827, Switzerland) was used for pH determinations. A centrifuge (HP190, Iran), Samsung microwave (Samsung, SAMI6, South Korea) and x-ray diffraction (XRD) (Rigaku D-maxCIII, Japan), with a Cu- Kα radiation source using Ni-filtered, was used. Morphological studies of MOF surface were studied by the scanning electron microscope (SEM) (JEOL JSM-6700F, Japan).

2.3. Preparation and synthesis of nanostructures of Zr-MOF

Synthesis of Zr-MOF was performed by micellation and microwave methods. Briefly, 0.6 g of zirconium sulfate and 0.5 g of 2,6- pyridine dicarboxylic acid ammonium were dissolved in 10 ml distilled water. After 15 min, 5 ml of 0.4 g CTAB solution in 50 ml of distilled water was added to the reaction. After 50 min, 0.8 g of sodium hydroxide was dissolved in 50 ml of distilled water and then, after 30 min, 0.5 g of thiourea was added to 5 ml of this solution in order to stabilize and create an electrostatic space. After 20 min, the mixture was put into the microwave at 450 MW for 10 min. After centrifugation, the precipitate was dried at room temperature. The Microwave conditions for synthesis of zirconium metal-organic framework nanostructures are shown in Table 1.

Table 1. Microwave conditions for synthesis of Zr-MOFs nanostructures

Sample	Power (watt)	Time (Minutes)	Size (nm)
A	450	5	230
B	450	10	350
C	600	5	210
D	600	10	300

2.4. Preparation of Zr-MOF/MIP film modified sensor

Prior to modification, bare GCE was thoroughly polished on, the surface of GCE was polished with aqueous slurry of alumina powder until a mirror like finish was obtained and then thoroughly washed with distilled water. Then, 0.01 g of Zr-MOF was dissolved in phosphate buffer solution, then the solution was deposited by electropolymerization on GCE surface, by employing CV in the potential range of -1.0 to +1.5 V with 10 cycles and scan rate of 50 mVs^{-1}. For designing a selective Molecularly imprinted cavity, 1.0 mM template molecule (DFC), 5 mM monomer (pABA) and 0.1 M phosphate buffer (pH=7, 0.1 M) as the supporting electrolyte was electrodeposited on the surface of Zr-MOF/GCE, using potential cycling between -1.0 and +1.5 V cycles for 15 cycles. Before polymerization, to remove dissolved oxygen, the solution was purged with high purity nitrogen for 5 min. After MIP synthesis using electropolymerization, template was removed from the polymers with 50% (v/v) methanol/acetic acid solution, on a magnetic stirrer at 150 rpm for 10 min. A sample of non-imprinted polymers (NIPs), were prepared under similar condition, but in the absence of the template and used for comparison of specificity.

2.5. Electrochemical measurements

Due to the lack of electrochemical activity of DFC in the potential range of the assay, an electroactive species of ferrocyanide was used as a probe. Electrochemical measurements were performed in the presence of solution of ferrocyanide of 2.0 mM and sodium sulfate of 0.2 mM in the potential range of -0.6 to 1.0 V, with a scan rate of 50 mVs^{-1} by cyclic voltammetry (CV). Differential pulse voltammetry methods (DPV) runs for each concentration of test analyte were quantified over a potential range of -0.6 to 1.0 V at a scan rate of 20 mVs^{-1} and pulse amplitude of 50 mV.

3. RESULTS AND DISCUSSION

3.1. Morphology and characterization of Zr-MOF

To study of the synthesized zirconium metal-organic framework nanostructures, its scanning electron microscope (SEM) image is shown. SEM is used to collect structural, chemical, and morphological information from nano particles (NPs) at atomic or nanometer scales. The sample surface of the nanostructures and, as can be seen in Fig. 1, the particle size is about 30 nm.

The X-ray diffraction (XRD) pattern of the nanostructures is shown in Fig. 2. As can be seen, the crystalline plates are well formed and the sample has high crystallinity. The size of the nanoparticles is in good agreement with the microscopic images and is calculated by the Debye-Scherrer equation and by calculating the width cycle at half maximum at about 50 nm.

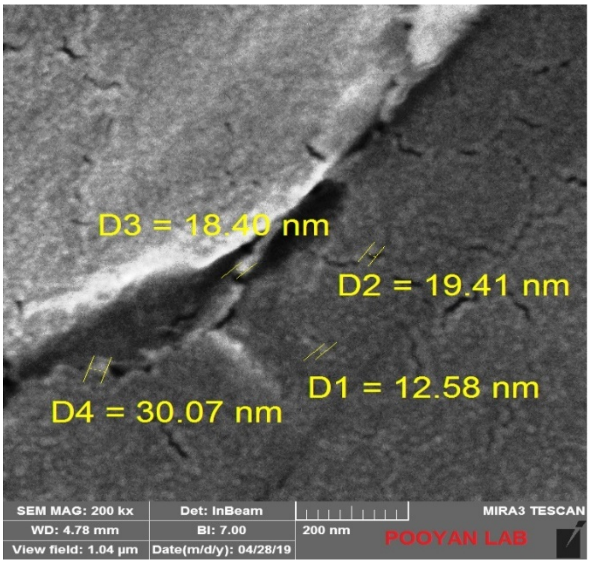

Fig. 1. Scanning electron microscopy image of Zr-MOFs nanostructures

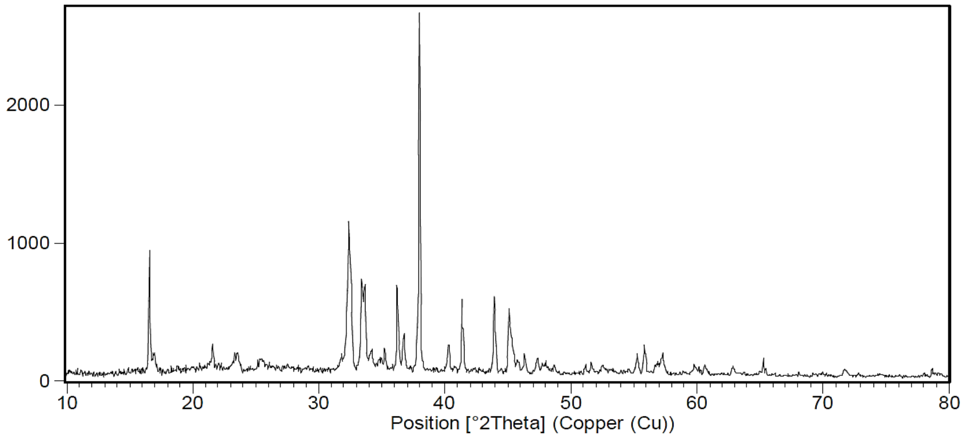

Fig. 2. XRD pattern of zirconium metal-organic framework nanostructures

3.2. Electrochemical behavior of DFC at the modified GCE surface

Cyclic voltammetry method was used to characterize the electrochemical behavior of the imprinted sensor. The cyclic voltammogram of the bare GCE, MIP/GCE, NIP/GCE, Zr-MOF/MIP/GCE and Zr-MOF/NIP/GCE in the 2.0 mM [$K_4[Fe(CN)_6]$] solution as a probe and 0.2 M Na_2SO_4 as redox probe are reported (Fig 3). (curve a) represents a pair of oxidation and reduction peak of probe on the bare GCE. When the template removal process is performed on MIP/GCE, NIP/GCE, Zr-MOF/MIP/GCE and Zr-MOF/NIP/GCE electrodes, no change in NIP/GCE electrode behavior (curve b) and Zr-MOF/NIP (curve c), was observed. But in the MIP/GCE electrode, redox peak related to probe, observed weakly (curve d). The Zr-MOF/MIP synthesis on the surface of the electrode, the surface-to-volume ratio should be increased. This is well illustrated this fact that the removal of the template from the polymer matrix with metal-organic framework creates a recognition sites or holes that so probe can pass and reach to the electrode surface to perform the electrochemical process (curve e). When MIP/GCE, NIP/GCE, Zr-MOF/MIP/GCE and Zr-MOF/NIP/GCE electrodes, are rebounded by template, there is no change in the electrode behavior NIP/GCE (curve f) and Zr-MOF/NIP/GCE in the probe (curve g), but in MIP/GCE (curve h) and Zr-MOF/MIP/GCE (curve i), peaks of the probe disappear again. That means the MIP film has been made compact enough, and the probe anions could not reach to the electrode surface.

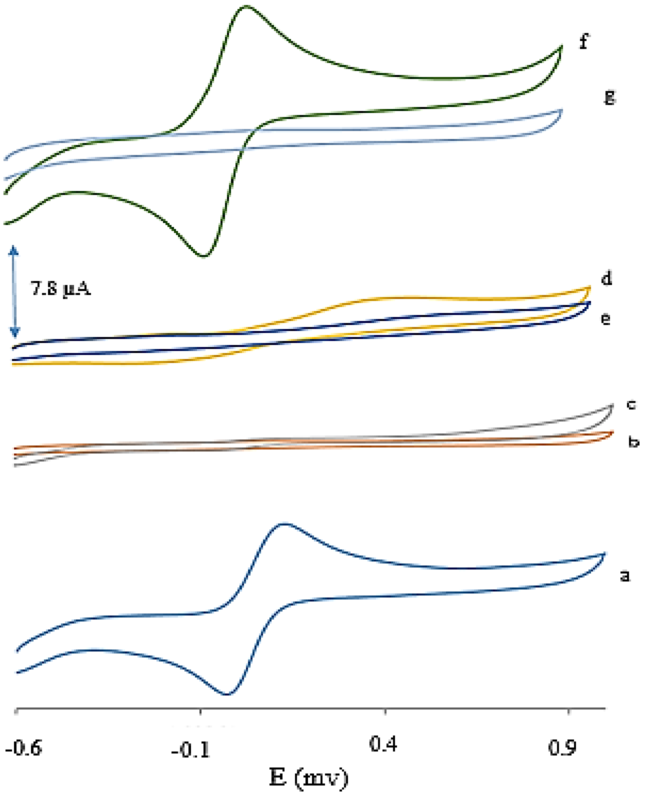

Fig. 3. The cyclic voltammograms of the different electrodes in the 2.0 mM Fe(CN)$_6$ solution and 0.2 M Na$_2$SO$_4$ with scan rate of 50 mVs^{-1}. (a) bare GCE, (b) NIP/GCE and (c) Zr-MOF/NIP/GCE after removal, (d) MIP/GCE and (e) Zr-MOF/MIP/GCE after DFC removal, (f) NIP/GCE and (g) Zr-MOF/NIP/GCE after DFC rebinding, (h) MIP/GCE and (i) Zr-MOF/MIP/GCE after DFC rebinding

3.3. Optimization of the parameters influencing Zr-MOF/MIP/GCE

Optimization of analytical parameters in order to achieve the best efficiency, for the designed sensor was divided into six sections including: optimization of the concentration of monomer (pABA), template (DFC) concentration, solution pH, the number of scans in polymerization step, study of template molecule remove, and the potential applied and time for rebinding of template on Zr-MOF/MIP/GCE.

The monomer concentration during the electropolymerization affects the thickness of the deposit and the amount of imprinted molecule in the polymer matrix, which in turn further affects the electrochemical behavior of the sensor. To evaluate the effect of the pABA concentration on the response of MIP/MOF/GCE sensor to DFC, the MIPs were electropolymerized in solutions of a constant DFC concentration (0.5 mM) and of varying pABA concentrations in the range of 0.5-7.0 mM by cycling the potential between -0.6 to 1.0 V was studied in our investigation. The results are shown in Fig. 4A. As a result, the response of the Zr-MOF/MIP/GCE to DFC increases with increasing the concentration of pABA up to 5.0 mM, then it decreased when the pABA concentration increased further, which was probably because the imprinted polymer membranes are too thick due to high concentration of pABA (above 5.0 mM), template molecules situated at the central area of the polymer membranes cannot be completely removed from polymer matrix. Thus, the optimum concentration 5.0 mM pABA was selected for further work.

The quality and quantity of diagnostic sites of MIPs are directly dependent on the mechanisms and extent of interaction between the template molecule and the monomer present in the pre-polymerization solution. According to the results in Fig. 4B. The highest changes of current response were observed in concentration 1.0 mM of DFC. Low concentrations of the DFC molecule decrease the sensitivity of the sensor, the number of recognition sites, the current changes and more value of template molecules also damage to the formation of polymer film. Therefore, a concentration of 1.0 mM, was selected as the optimum concentration for synthesis of the Zr-MOF/MIP/GCE polymer film.

The effect of solution pH was investigated because that is one of the important reasons for the recognition of imprinted molecules in electrostatic interactions. To find the optimum solution pH, the influence of pH (between 3.5 and 10.0, using phosphate buffers) on peak current was studied (Fig. 4C). The maximum peak current was obtained in pH 7 and thus this pH was selected for subsequent uses.

The number of CV cycles could influence the thickness of the imprinted polymers, which would influence the sensitivity and stability of the sensor Fig 4D. It was carried out in 6 to 20 cycles to study this experiment parameter. The current response reached maximum with 15 cycles, and then decreased with further increasing of cycle number. Generally, if the imprinted polymer membranes are too thick, MIP film may hinder the accessibility of templates molecules to the imprinted sites and a fine MIP film could be broken conveniently. Similarly, the compactness of the MIP membranes affected by the scan rate of the electropolymerization would influence the mass transfer of the template and further influence the sensitivity of the MIP sensor.

After electrosynthesis, template must be removed in order to create imprinting cavities. Different extraction solvents were used for this purpose. Initially, the imprinted polymer film in phosphate buffer solution for 30 min was used to remove the template molecule and it was found that this solution be ineffective for template removal. In addition, the use of 0.1 M HCl in template removal was also unsuccessful.

Then ethanol and methanol organic solvents were used to remove the template, that methanol was able to partially remove the template. It was found that, by the electro-polymerization method the Zr-MOF/MIP sensor was immersed in 50% (v/v) methanol/acetic acid solution at room temperature for 10 min, to remove the imprinting molecule. This is due to the good solubility of DFC in methanol/acetic acid solution.

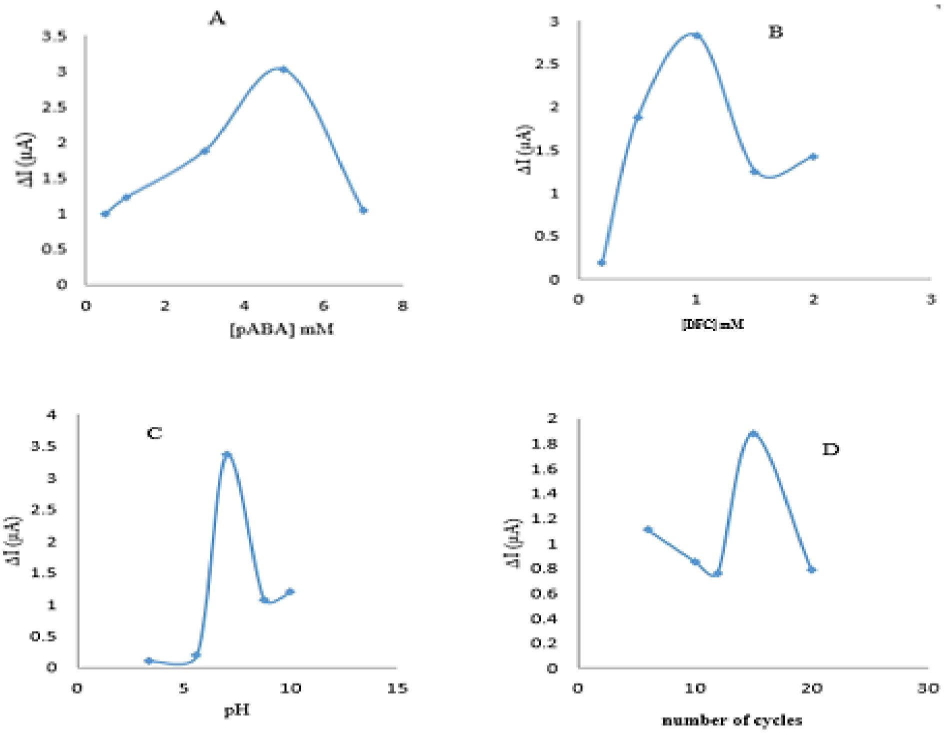

Fig. 4. Optimization of factors affecting the performance of the Zr-MOF/MIP/GCE ; effects of: (A) pABA, and (B) diclofenac concentrations (C) pH, and (D) the number of CVs on Zr-MOF/ MIP synthesis

3.4. Electrochemical response of the Zr-MOF/MIP sensor

The calibration curve was plotted to determine the DFC linear range and the limit of detection. Differential pulse voltammograms at different concentrations of the template molecule in the ferrocyanide probe were recorded to plot the calibration curve under optimization conditions. The imprinted sites were occupied with increasing the concentration of template molecule according to (Fig. 5A), and the probability of the ferrocyanide probe for reaching to the electrode surface is reduced, therefore the current is reduced. The calibration curve was plotted based on the current changes and the concentration of the template molecule, according to the recorded voltammograms. The linear range of 6.5 µM to $1.5\times10^{+3}$ µM, with the regression equation being $\Delta I=0.0058+0.9877$ ($R^2=0.9986$) according to the results shown (Fig. 5B). The limit of detection (LOD), which is determined according to $3S_b/m$, where b is the standard deviation for 6 measurements, and m is the slope of calibration curve, was determined to be as low as 0.043 µM. The repeatability of the method was determined by the relative standard deviation (RSD). For this purpose, RSD by recording the responses of DPV, at seven measurements of Zr-MIP/MOF/GCE modified electrodes at a specific concentration of 1.0 mM DFC was calculated as 1.8%, which indicates the good repeatability of sensor. The prepared Zr-MIP/MOF/GCE sensor was stored at room temperature, and was used every day to evaluate the same DFC concentration. After one-month, were observed without obvious decrease.

For possible analytical application of the method, the effects of some common interferences on the determination of 0.5 mM DFC was examined. The tolerance limit was defined as the maximum concentration of the substances that caused an error of less than 5% in DFC determination. 100-fold concentration of mefenamic acid, glucose, ascorbic acid and maleic acid, have no influence on the current response of DFC upon the experimental conditions.

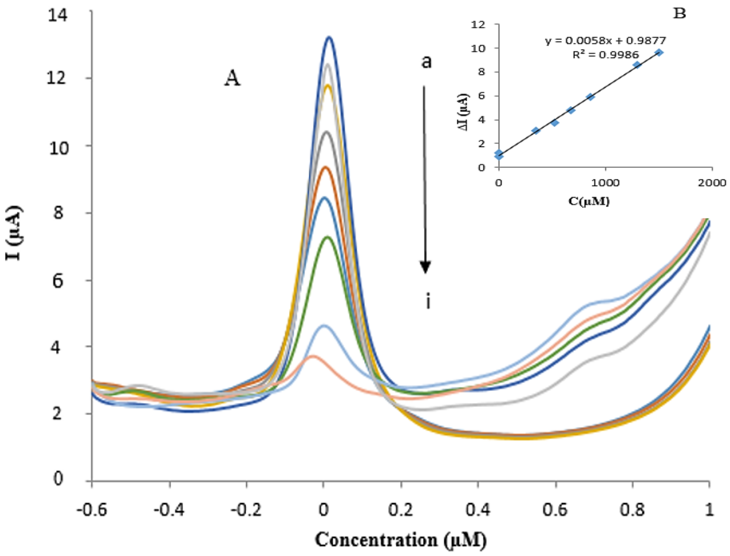

Fig. 5. DPVs of the Zr-MOF/MIP/GCE in various concentrations of DFC solution, a to i: 0, 6.5, 350, 520, 670, 857, 1300 and 1500 µM, and the related calibration curve

3.5. Analysis of real samples

To verify applicability of the sensor in real sample detection, a DFC tablet containing 5 mg DFC was dissolved in phosphate buffer with pH=7 and subsequently, the DFC content in the drug sample was determined using a modified Zr-MIP/MOF/GCE by standard addition method. The analytical results in Table 2 are shown good accuracy with recovery values ranging from 101.3 to 102.2%. The obtained recoveries indicated that the modified electrode could be successfully used for the determination of DFC in pharmaceutical sample.

Table 2. Results for the determination of DFC in Alfen X tablet

Sample	Added (µM)	Detected (µM)	Recovery (%)	RSD (%)
1	-	4.5×10^{-1}	-	2.1
2	4.7×10^{-1}	9.0×10^{-1}	102.2	2.1
3	6.2×10^{-1}	1.5	101.3	4.1
4	7.8×10^{-1}	2.2	102.2	3.0

4. CONCLUSION

A new sensor based on Zr-MOF/MIP/GCE was synthesized by electropolymerization method for highly sensitive and selective detection of DFC. Initially, the thin layer coating of zirconium metal-organic frameworks and molecularly imprinted polymer were deposited on the surface of the glass carbon electrode and Zr-MOF/MIP sensor was prepared. The advantages of this method are its high selectivity, long term stability, low cost, and the presence of Zr-MOFs nanostructures due to its high active surface, which increases the sensitivity of DFC. The analytical characteristics of the present sensor were compared with other works that have been reported for determination of DFC and the results are presented in Table 3. As can be seen, the proposed sensor has the linear range and relative standard deviation comparable or better detection limit relative to other reported works. The proposed sensor was used successfully for diclofenac determination in the real sample.

Table 3. Comparison of Zr-MIP/MOF/GCE sensor with other reported methods for the determination of Diclofenac

Method	Linear range (µM)	Detection limit (µM)	Recovery (%)	RSD (%)	Ref.
TCPE	10-140	3.28	98.8-99.3	3.50	[42]
NHMN	196-2650	31.7	101	5.42	[43]
f-MWCNTs-GO/ AuNPs/AuE	0.4-1000	0.09	98.8-105	2.80	[44]
GO-COOH-GCE	1.2-400	0.09	92.9-93.2	2.56	[45]
Au–PtNPs/f-MWCNTs/AuE	1000 -0.5	0.30	98-102	1.70	[46]
MIP/GCE/Zr-MOF	6.5-1500	0.1	101.3-102.2	1.8	This work

Acknowledgment

We gratefully acknowledge the partial support of this work from the Department of Chemistry, Payame Noor University Tehran, Iran.

REFERENCES

[1] R. N. Goyal, S. Chatterjee, and A. R. S. Rana, Carbon 48 (2010) 4136.
[2] R. N. Goyal, S. Chatterjee, and B. Agrawal, Sens. Actuators B Chem. 145 (2010) 743.
[3] J. B. Quintana, J. Carpinteiro, and I. Rodríguez, Compr. Anal. Chem. 50 (2007) 185.
[4] W. Schneider, and P. Degen, J. Chromatogr. A. 217 (1981) 263.
[5] Á. Sebők, A. Vasanits-Zsigrai, G. Palkó, G. Záray, and I. Molnár-Perl, Talanta 76 (2008) 642.
[6] A. ÁARMT, and V. J. V. J. M. Cortés, Chromatography online 37 (2019) 194.
[7] M. M. Mabrouk, S. F. Hammad, F. R. Mansour, and B. Z. El-Khateeb, J. Anal. Chem. 74 (2019) 458.
[8] R. V. Mane, K. Patel, G. S. Sushmitha, and S. Vasantharaju, Res. J. Pharm. Technol. 12 (2019) 611.
[9] E. M. Thalij, S. A. Salman, and H. M. Hasan, Tikrit J. Pure Sci. 24 (2019) 52.
[10] P. R. Barros Gomes, V. E. Mouchrek Filho, S. de Oliveira, R. Wesly, A. Pereira Everton, J. Batista Reis, H. C. Louzeiro, W. da Silva Lyra, M. A. Fontenele, and D. T. Valeriano Alveset, Rev. Colomb. Cienc. Quim. Farm. 48 (2019) 29.
[11] O. Corcoran, J. K. Nicholson, E. M. Lenz, F. Abou-Shakra, J. Castro-Perez, A. B. Sage, and I. D. Wilsonet, Rapid Commun. Mass Spectrom. 14 (2000) 2377.
[12] N. K. Sahoo, M. Sahu, P. S. Rao, and G. Ghosh, J. Anal. Chem. 70 (2015) 424.
[13] L. Nováková, D. Solichová, and P. Solich, J. Sep. Sci. 29 (2006) 2433.
[14] U. Geiger, P. Degen, and A. Sioufi, J. Chromatogr. A 111 (1975) 293.
[15] L. González, G. Yuln, and M. Volonté, J. Pharm. Biomed. Anal. 20 (1999) 487.
[16] R. Hajkova, P. Solich, M. Pospıšilová, and J. Šıcha, Anal. Chim. Acta 467 (2002) 91.
[17] Y. M. El-Sayed, M. E. Abdel-Hamed, M. S. Suleiman, and N. M. Najib, J. Pharm. Pharm. 40 (1988) 727.
[18] L. Zecca, P. Ferrario, and P. Costi, J. Chromatogr. B Biomed. Sci. Appl. 567 (1991) 425.
[19] V. Dighe, R. Sane, S. Menon, H. Tambe, S. Pillai, and V. Gokarn, JPC-J. Planar Chromat. 19 (2006) 443.
[20] E. Kaale, B. C. Nyamweru, V. Manyanga, M. Chambuso, and T. Layloff, Int. J. Chem. Anal. Sci. 4 (2013) 73.
[21] W. Thongchai, B. Liawruangrath, C. Thongpoon, and T. Machan, Chiang Mai J. Sci. 33 (2006) 123.
[22] C. Sarbu, M. Demertzis, and D. Kovala-Demertzi, Acta Chromatographica. 10 (2000) 222.

[23] M. S. García, M. I. Albero, C. Sánchez-Pedreño, and J. Molina, J. Pharmaceut. Biomed. Anal. 17 (1998) 267.

[24] S. García, C. Sánchez-Pedreño, I. Albero, and C. García, Microchim. Acta 136 (2001) 67.

[25] J. Perlado, A. Zapardiel, E. Bermejo, J. Perez, and I. Hernandez, Anal. Chim. Acta 305 (1995) 83.

[26] A. Samadi-Maybodi, S. K. H. Nejad-Darzi, and H. Ilkhani Anal. Bioanal. Electrochem. 3 (2011) 134.

[27] F. Huang, G. Jin, Y. Liu, and J. Kong, Talanta 74 (2008) 1435.

[28] Y-H. Zhu, Z-L. Zhang, W. Zhao, and D-W. Pang, Sens. Actuators B Chem. 119 (2006) 308.

[29] K. Li, M. Zhu, H. Zhang, and J. Zhao, Int. J. Electrochem. Sci. 8 (2013) 4047.

[30] A. Poma, H. Brahmbhatt, J. K. Watts, and N. W. Turner, Macromolecules 47 (2014) 6322.

[31] J. Wackerlig, and R. Schirhagl R. Anal. Chem. 88 (2015) 250.

[32] F. Puoci, G. Cirillo, M. Curcio, O. I. Parisi, F. Iemma, and N. Picci, Expert Opin. Drug Deliv. 8 (2011) 1379.

[33] K. Eersels, B. V. Grinsven, M. Khorshid, V. Somers, C. Püttmann, C. Stein, S. Barth, H. Diliën, G. M. J. Bos, W. T. V. Germeraad, T. J. Cleij, R. Thoelen, W. De Ceuninck, and P. Wagner, Langmuir 31 (2015) 2043.

[34] S. Mohamed, S. Balieu, E. Petit, L. Galas, D. Schapman, J. Hardouin, R. Baati, and F. Estour, Chem. Commun. 55 (2019) 13243.

[35] M. Resmini, Anal. Bioanal. Chem. 402 (2012) 3021.

[36] G. Ertürk Bergdahl, T. Andersson, M. Allhorn, S. Yngman, R. Timm, and R. Lood, ACS Sens. 4 (2019) 717.

[37] M. L. Yola, and N. Atar, Biosens. Bioelectron. 126 (2019) 418.

[38] A. Herrera-Chacón, S. D. Zor, and M. D. Valle, Talanta 208 (2019) 120348.

[39] A. Sinha, S. M. Mugo, X. Lu, and J. Chen, Tools, Techniques and Protocols for Monitoring Environmental Contaminants: Elsevier (2019) pp. 371.

[40] K. Orihara, A. Hikichi, T. Arita, H. Muguruma, and Y. Yoshimi, J. Pharm. Biomed. Anal. 151 (2018) 324.

[41] L. Fernández-Llano, M. C. Blanco-López, M. J. Lobo-Castañón, A. J. Miranda-Ordieres, and P. Tuñón-Blanco, Electroanalysis 19 (2007) 1555.

[42] B. Chethana, S. Basavanna, and Y. Arthoba Naik, Ind. Eng. Chem. Res. 51 (2012) 10287.

[43] M. Hajjizadeh, A. Jabbari, H. Heli, A. Moosavi-Movahedi, and S. Haghgoo, Electrochim. Acta 53 (2007) 1766.

[44] F. Nasiri, G. H. Rounaghi, N. Ashraf, and B. A. Deiminiat, Int. J. Environ. Anal. Chem. 1 (2019) 1.

[45] C. Karuppiah, S. Cheemalapati, S. M. Chen, and S. Palanisamy, Ionics 21 (2015) 231.

[46] M. M. Eteya, G. H. Rounaghi, and B. Deiminiat, Microchem. J. 144 (2019) 254.